

Effect of Acoustic Nonlinearity on Heating of Biological Tissue by High-Intensity Focused Ultrasound

E. A. Filonenko and V. A. Khokhlova

Moscow State University, Vorob'evy gory, Moscow, 119899 Russia

e-mail: vera@acs366b.phys.msu.su

Received June 22, 2000

Abstract—Effect of strong acoustic nonlinearity on the efficiency of heating of a biological tissue by high-intensity focused ultrasound in the modes of operation used in real clinical setups is studied. The spatial distributions of thermal sources and the corresponding temperature increments caused by ultrasonic absorption are analyzed. Numerical algorithms are developed for simulating the nonlinear focusing of ultrasound in the calculations of both the heat sources on the basis of the Khokhlov–Zabolotskaya–Kuznetsov-type equations and the temperature field in a tissue on the basis of an inhomogeneous thermal conduction equation with a relaxation term. It is demonstrated that in the mode of operation typical of acoustic surgery, the nonlinearity improves the locality of heating and leads to an increase in the power of thermal sources in the focus by approximately an order of magnitude. The diffusion phenomena in the tissue lead to a smoothing of the spatial temperature distributions, as compared to the distributions of thermal sources. In the case of one-second exposure in the nonlinear mode of focusing, the maximal temperature in the focus exceeds the values obtained in the approximation of linear wave propagation by a factor of three. © 2001 MAIK “Nauka/Interperiodica”.

Utilization of high-intensity ultrasound for therapy is a rapidly developing field of modern medical science [1–4]. One of the mechanisms of ultrasonic action on a tissue is its heating due to the absorption of the energy of the ultrasonic waves. The thermal mechanism is used in two modes of operation. The first mode is a hyperthermic one when the tissue is affected by low-intensity ultrasound of about 1–10 W/cm² during 30–60 min, which provides the heating of the tissue up to 42–45°C [2]. However, it is difficult to maintain the temperature within the necessary narrow range during the total time of exposure. An alternative is the mode with high-intensity but short-time irradiation. In this mode called acoustic surgery, the irradiation of a tissue is performed over several seconds using an intense focused ultrasonic beam with the intensity in the focus 500–2000 W/cm². In this case, localization of the heated region and a rapid increase in temperature up to 60–90°C, which causes the necessary destruction of the tissue, are obtained. For example, the mode of acoustic surgery can be used for therapy of cancerous growths [3, 4].

The effects of acoustic nonlinearity start to play a considerable role in the case of such a high ultrasonic intensity. They lead to the appearance of additional higher harmonics in the initial wave spectrum, the formation of shock fronts in the wave profile, and, correspondingly, the increase in the absorption of the ultrasonic wave energy and in the efficiency of tissue heating [5–8]. Despite the fact that the nonlinear effects in the diagnostic and therapeutic applications of ultrasound have been greatly studied (see the review in [5]),

they are rarely taken into account in calculating the irradiation doses and the parameters of ultrasonic setups in real clinical experiments, and they are almost never used for the optimization and increasing the efficiency of heating. The purpose of this work is the investigation of the effects of acoustic nonlinearity in the process of the tissue heating by a high-intensity focused ultrasonic beam in the modes of operation characteristic of real clinical setups [3, 7].

The problem is divided into two parts in order to develop a theoretical model of the heating process. In the first part, the nonlinear propagation of a focused acoustic beam in a tissue is studied and the spatial distribution of thermal sources is calculated. In the second part, the temperature field is calculated for the known distribution of sources. The acoustic field is simulated for the case of a piston piezoelectric radiator with the radius $r_0 = 4.2$ cm, the focal distance $F = 15$ cm, and the frequency $f_0 = 1.7$ MHz (Fig. 1), which is used in the ultrasonic clinical setup at the Institute of Cancer Studies in Sutton [7]. The power of the source is selected in such a way that the field intensity in the focus calculated in the linear approximation is $I_F = 1500$ W/cm². It was found experimentally that in the case of the time of ultrasonic irradiation about 1 s, this mode provides the necessary destruction of soft tissues [3]. With the radiator intensity determined in such a way, the calculation of the acoustic field, the thermal sources, and the temperature field is performed both taking and not taking into account the effects of acoustic nonlinearity. The comparison of the simulation results for these two cases provides an opportunity to obtain the quantitative esti-

mates of the role of acoustic nonlinearity in the efficiency of thermal action of ultrasound upon a tissue.

ACOUSTIC FIELD

The propagation of an intense focused acoustic wave in a tissue is described in the parabolic approximation by the nonlinear evolution equation of the Khokhlov–Zabolotskaya–Kuznetsov type [8]

$$\frac{\partial}{\partial \tau} \left[\frac{\partial p}{\partial z} - \frac{\varepsilon}{c_0^3 \rho_0} p \frac{\partial p}{\partial \tau} - L_{\text{abs}} p \right] = \frac{c_0}{2} \Delta_{\perp} p, \quad (1)$$

where p is the acoustic pressure in the beam; z is the coordinate along the beam axis; $c_0 = 1614$ m/s is the propagation velocity of longitudinal acoustic waves in the tissue; $\rho_0 = 1214$ kg/m³ is the equilibrium density; $\varepsilon = 4.78$ is the nonlinearity factor of the tissue [7]; $\tau = t - z/c_0$ is the time in the moving coordinate system; and Δ_{\perp} is the Laplacian with respect to the transverse coordinates, which, in the case of an axisymmetric beam considered here, has the form $\Delta_{\perp} = \partial^2/\partial r^2 + 1/r \partial/\partial r$. The linear operator L_{abs} describes the absorption of a wave in compliance with the power law characteristic of biological tissues:

$$\alpha(f) = \alpha_0 (f/f_0)^{\eta}, \quad (2)$$

where the power index η is close to unity, α is the absorption coefficient at a frequency f , and α_0 is the absorption coefficient at the selected frequency f_0 [2]. For a tissue of liver type, the values of the parameters η and α_0 at the selected radiation frequency 1.7 MHz are equal to $\eta = 1.266$ and $\alpha_0 = 8.42$ m⁻¹ [7], respectively. Equation (1) takes into account the nonlinear, dissipative, and diffraction effects.

In the case of a focused piston radiator under study, we have

$$p(z=0, r, \tau) = \begin{cases} p_0 \sin[\omega_0(\tau + r^2/2c_0F)], & r \leq r_0 \\ 0, & r > r_0 \end{cases} \quad (3)$$

and an exact analytical solution for the acoustic field can be obtained only at the beam axis and in the focal plane $z = F$ in the linear approximation. It is impossible to obtain an analytical solution for the field in the whole space. Therefore, in order to determine the spatial distribution of thermal sources, the acoustic field of the radiator given by Eq. (3) is simulated numerically in the case of both linear and nonlinear propagation of waves.

Several approaches had been developed for the numerical solution of the problem of the focusing of intense acoustic beams. They use either the temporal finite-difference schemes of a direct integration of equations of the type of Eq. (1) [9–11] or the spectral schemes based on solving a system of coupled nonlinear equations for the amplitudes of the harmonics of the initial wave [7–9, 12–16]. The temporal approach is

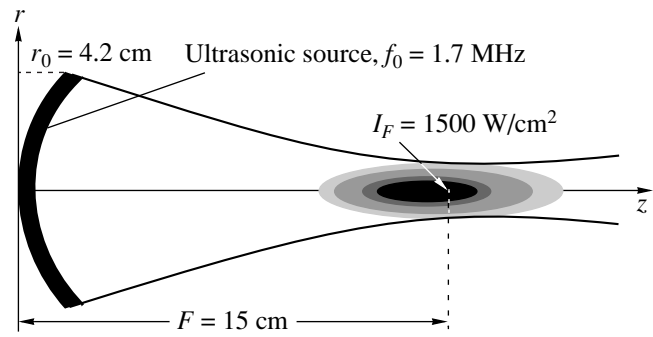


Fig. 1. Geometry of the problem.

more suitable for investigating the focusing of pulses [10, 11], and the spectral approach is more suitable for describing periodic waves [12–16], as well as in the case when the frequency power law governing the absorption in the medium differs from the quadratic one and the operator L_{abs} in Eq. (1) has an integral form. In this paper, we use the spectral approach.

In order to construct a numerical algorithm, we change to dimensionless variables in Eq. (1):

$$\frac{\partial}{\partial \theta} \left(\frac{\partial P}{\partial Z} - NV \frac{\partial P}{\partial \theta} - AL_{\text{abs}} P \right) = \frac{1}{4G} \left(\frac{\partial^2 P}{\partial R^2} + \frac{1}{R} \frac{\partial P}{\partial R} \right). \quad (4)$$

Here, $P = p/p_0$ is the acoustic pressure normalized to the initial amplitude p_0 at the source; $\theta = \omega_0 \tau$ is the dimensionless time, where $\omega_0 = 2\pi f_0$; $Z = z/F$ is the propagation coordinate normalized to the focal length; and $R = r/r_0$ is the transverse coordinate normalized to the radiator radius. Three dimensionless parameters, namely, N (nonlinearity), G (diffraction), and A (absorption),

$$N = \frac{F}{z_n}, \quad G = \frac{z_d}{F}, \quad A = \frac{F}{z_a}, \quad (5)$$

characterize the relations between the four characteristic spatial scales of the problem: the focal length F , the diffraction length $z_d = \omega_0 r_0^2 / 2c_0$, the length of shock formation $z_n = c_0^3 \rho_0 / \varepsilon \omega_0 p_0$, and the absorption length for the radiation frequency $z_a = \alpha_0^{-1}$. Then, the boundary condition given by Eq. (3) can be represented in the form

$$P(Z=0, R, \theta) = \begin{cases} \sin(\theta + GR^2), & R \leq 1 \\ 0, & R > 1. \end{cases} \quad (6)$$

The values of the dimensionless parameters of diffraction and absorption, which are determined by Eq. (5), are equal to $G = 38.7$ and $A = 1.25$, respectively. We use the exact solution to the linearized Eq. (4) at the beam

axis for a piston radiator (Eq. (6)) to estimate the intensity at the source $I_0 = p_0^2/2c_0\rho_0$ according to the intensity $I_F = 1500 \text{ W/cm}^2$ preset in the focus at $Z = 1$:

$$I(Z, R = 0) = \frac{4I_0}{(1-Z)^2} \sin^2\left(G\frac{1-Z}{2Z}\right) \exp(-2AZ). \quad (7)$$

Setting $Z = 1$ in Eq. (7), we obtain $I_0 = I_F \exp(2\alpha_0 F)/G^2 = 12 \text{ W/cm}^2$, which corresponds to the pressure amplitude $p_0 = 0.7 \text{ MPa}$ and the value of the nonlinearity parameter $N = 1.07$. The parameter N is taken equal to zero in calculating the linear focusing.

We seek the solution to Eq. (4) in the form of the Fourier series expansion:

$$P(Z, R, \theta) = \sum_{n=-\infty}^{\infty} C_n(Z, R) \exp(-in\theta), \quad (8)$$

where C_n is the complex amplitude of the n th harmonic in the spectrum of a propagating wave. Substituting expansion (8) into Eq. (4), we obtain a set of coupled equations for the amplitudes of harmonics

$$\begin{aligned} \frac{\partial C_n}{\partial Z} &= \frac{i}{4n} \Delta_{\perp} C_n - \frac{in}{2} \sum_{k=-\infty}^{\infty} C_k C_{n-k} \\ -K''(n)C_n + iK'(n)C_n &= L_{\text{diff}}^{(n)} + L_{\text{nonl}}^{(n)} + L_{\text{abs}}^{(n)}, \end{aligned} \quad (9)$$

where $L_{\text{diff}}^{(n)}$, $L_{\text{nonl}}^{(n)}$, and $L_{\text{abs}}^{(n)}$ are the operators describing the diffraction, nonlinear, and dissipative phenomena for the n th harmonic, respectively, and K' and K'' are the dimensionless real and imaginary parts of the wave number; the latter quantities have the following form in the moving coordinate system:

$$\begin{aligned} K(n) &= k(nf_0)F = K' + iK'', \\ K''(n) &= \alpha(nf_0)F = An^n, \\ K'(n) &= 2\pi n f_0 (1/c(nf_0) - 1/c_0)F \\ &= A \frac{2n}{\pi(\eta - 1)} (1 - n^{\eta-1}). \end{aligned} \quad (10)$$

The frequency dependence of the absorption K'' is simulated by Eq. (2), and the dispersion of sound velocity K' is calculated according to the known dependence (2) using local dispersion relations of the Kramers–Kronig type [17].

The numerical integration of Eqs. (9) is conducted for a finite number of the first harmonics n_{max} . For $n > n_{\text{max}}$, the amplitudes C_n are assumed to be zero. To provide the stability of the numerical scheme at the stage of the developed shocks, an additional artificial viscosity proportional to the squared frequency is introduced: $K''(n)_{\text{art}} = A_1 n^2$. Since biological tissues consist mainly of water, the coefficient A_1 is selected to be equal to the absorption coefficient in water $\alpha_w(f_0) = 7.23 \times 10^{-4} \text{ cm}^{-1}$: $A_1 = 1.08 \times 10^{-2}$.

The method of splitting in the physical factors is used at each step of integration along the axis from the layer Z to the layer $Z + hZ$. This technique is realized in three stages. At the first stage, the diffraction effects described by the operator L_{diff} are taken into account for each harmonic. An absolutely implicit difference scheme is used at the distances close to the radiator, and after that, the Crank–Nicholson scheme is used [18]. The solution obtained for the diffraction problem at a new layer $Z + hZ$ is taken as the initial condition for the second stage of taking into account of the nonlinear effects described by the system of coupled nonlinear equations $\partial C_n/\partial Z = L_{\text{nonl}}$. The system is solved for each node of the grid constructed in R by the Runge–Kutta method with the fourth-order precision [18]. The representation of the solution in the form of the Fourier series in a complex form (Eq. (10)) provides an opportunity to avoid the use of an iteration procedure in simulating the nonlinear operator. The necessity of this procedure arises in the case of the Fourier series expansion in the real form [12, 13]. The solution of the nonlinear problem is used as an initial one for the third stage when the dissipative phenomena described by the set of equations $\partial C_n/\partial Z = L_{\text{abs}}$ are taken into account. Here, the exact result $C_n(Z + hZ, R) = C_n(Z, R) \exp(hZ(-K''(n) + iK'(n) + iK'(n)))$ is used for each node of the grid and each harmonic.

From the determined amplitudes of harmonics, the intensity of each n th harmonic $I_n = 4|C_n|^2 I_0$, the total intensity of the wave

$$I(z, r) = \sum_{n=1}^{\infty} I_n(z, r), \quad (11)$$

and the power of thermal sources

$$q_v(z, r) = 2 \sum_{n=1}^{\infty} \alpha(nf_0) I_n(z, r), \quad (12)$$

where $\alpha(nf_0)$ is the absorption coefficient at the n th harmonic (Eq. (2)), are calculated.

The following values of the basic parameters of the scheme were used: the limits of integration with respect to the longitudinal coordinate $0 \leq Z \leq 1.8$, the spatial window in the transverse coordinate $0 \leq R \leq 2.5$, the step of the grid along the beam axis $hZ = 0.25 \times 10^{-4}$ for the implicit scheme and $hZ = 10^{-4}$ for the Crank–Nicholson scheme, and the step of the grid in the transverse coordinate $hR = 10^{-3}$.

The calculation of the focusing of an acoustic beam in a nonlinear mode when a shock front is formed in the wave profile needs rather long computer time. A variable number of harmonics $n(Z, R)$ is used to reduce the time of calculation in the scheme for different Z and R . The necessary number n is controlled in such way that when the amplitude of the last harmonic exceeds a certain preset value, the number of harmonics is gradually increased up to the maximal value $n_{\text{max}} = 1000$. Even

with such an optimization, the time of calculation for the nonlinear problem by a Dec Alpha XP 1000 computer was about 40 h.

One can see from Eq. (12) that a nonlinear transformation of the wave energy up the spectrum leads to an increase in the absorption of the ultrasonic wave energy because of the growth of the absorption coefficient with frequency (Eq. (2)). In the case of a strong manifestation of the nonlinear effects and the appearance of shocks in the wave profile, the heating of the tissue increases most strongly in the focal region. Let us consider some theoretical estimates. As is well known, the absorption at shocks does not depend on the value of the absorption coefficient of the medium and is determined by the wave amplitude and the value of the nonlinear parameter ε [5]. In the case of a linearly propagating harmonic wave, the heat release in the focus, $q_v = 2\alpha_0 I = 2\alpha_0 p_A^2 / 2c_0 \rho_0$, is proportional to the wave intensity or the squared pressure amplitude p_A , whereas in the case of the shock front formation, the heat release at the shock is proportional to the third power of its amplitude A_r :

$$q_{v, \text{shock}} = \frac{\omega_0 \varepsilon A_r^3}{2\pi 6c_0^4 \rho_0^2} = \frac{(A_r/p_A)^3 p_A^2}{12\pi z_n c_0 \rho_0}, \quad (13)$$

where $z_n = c_0^3 \rho_0 / \varepsilon \omega_0 p_A$ is the length of shock formation in a plane wave with the amplitude p_A . As one can see from Eq. (13), the ratio of absorption at the shock to its linear value is determined by the third power of the shock front amplitude and the ratio of the characteristic scales of absorption and nonlinearity in the tissue:

$$\frac{q_{v, \text{shock}}}{q_v} = \frac{(A_r/p_A)^3}{12\pi} \frac{1}{\alpha_0 z_n}. \quad (14)$$

We take into account in Eq. (14) that the shock amplitude in the focus can attain the value $3p_A$ due to the more effective focusing in the nonlinear mode [16] and calculate the nonlinear scale corresponding to the intensity 1500 W/cm^2 in the tissue. As a result, we obtain $z_n = 1.2 \text{ cm}$ and $q_{v, \text{shock}}/q_v = 7$. With allowance for the contribution of absorption at low frequencies given by Eq. (2), we can expect that, in the mode of developed shocks, the heating efficiency must increase by approximately an order of magnitude. The longitudinal dimension of the focal region of the considered radiator, which is determined by half the maximal intensity level (7), can be estimated approximately as $6F/G = 2 \text{ cm}$. Since the size of the focal region is greater than the length of shock formation z_n for a wave with the intensity $I_F = 1500 \text{ W/cm}^2$, we can expect that the mode of developed shocks is realized in the focus and the efficiency of the tissue heating is considerably increased.

TEMPERATURE FIELD

We use the inhomogeneous Pennes equation of heat conduction [19] to calculate the temperature field

$$\frac{\partial T}{\partial t} = k\Delta(T) - \frac{T - T_0}{\tau} + \frac{q_v}{c_v}, \quad (15)$$

where $T = T(\mathbf{r}, t)$ is the tissue temperature, $T_0 = 36.6^\circ\text{C}$ is the equilibrium temperature, $c_v = 3.81 \times 10^6 \text{ J}/(\text{C m}^3)$ is the heat capacity of a unit volume, $k = K/c_v = 1.3 \times 10^{-7} \text{ m}^2/\text{s}$ is the thermal diffusivity [7], K is the heat conductivity of the tissue, and Δ is the Laplacian. The first term on the right-hand side of Eq. (15) describes the process of diffusion, and the second term describes the cooling due to the intense heat transfer on account of the blood vessels present in both the heated region and outside it [2]. The characteristic time of the latter process for a liver-type tissue is equal to $\tau = \rho_b c_v / w c_{vb} = 250 \text{ s}$, where ρ_b , c_{vb} , and w are the density, the heat capacity, and the velocity of the blood flow, respectively [7]. The function $q_v(z, r)$ describes the field of thermal sources caused by the absorption of an ultrasonic wave (Eq. (12)). For a numerical simulation, it is convenient to reduce Eq. (15) to a dimensionless form:

$$\frac{\partial \tilde{T}}{\partial \tilde{t}} = \left[\alpha \frac{\partial^2}{\partial Z^2} + \beta \left(\frac{\partial^2}{\partial R^2} + \frac{1}{R} \frac{\partial}{\partial R} \right) \right] \tilde{T} - \frac{\tilde{T}}{\tau} + \gamma \tilde{q}(R, Z). \quad (16)$$

Here, $\tilde{t} = t/t_0$ is the time normalized to the characteristic heating time $t_0 = 1 \text{ s}$; $\tilde{T} = (T - T_0)/T_0$ is the dimensionless temperature normalized to the equilibrium value T_0 ; the dimensionless coefficients $\alpha = kt_0/F^2$ and $\beta = kt_0/r_0^2$ describe the diffusion along and across the beam axis, respectively; and $\gamma = I_0 t_0 F / (c_v T_0)$ is the dimensionless coefficient characterizing the power of the thermal sources.

As in the case of the acoustic field, we use the technique of splitting with respect to physical parameters in order to solve Eq. (16) numerically. At each time step $h\tilde{t}$ in passing from the time layer \tilde{t} to the layer $\tilde{t} + h\tilde{t}$, the problem is solved in two stages. At the first stage, the influence of the cooling process and the thermal sources is taken into account according to the equation $\partial \tilde{T} / \partial \tilde{t} = -\tilde{T} / \tau + \gamma \tilde{q}(R, Z)$, which has an exact solution

$$\begin{aligned} & \tilde{T}(\tilde{t} + h\tilde{t}) \\ &= \tilde{T}(\tilde{t}) \exp\left(-h\tilde{t} \frac{\tau_0}{\tau}\right) + \left[1 - \exp\left(-h\tilde{t} \frac{\tau_0}{\tau}\right)\right] \frac{\tau \gamma}{\tau_0} \tilde{q}. \end{aligned} \quad (17)$$

Solution (17) is taken as the initial temperature distribution for solving the diffusion part, which is approximated by the implicit longitudinal-transverse scheme providing the second-order precision in both time and spatial coordinates [18].

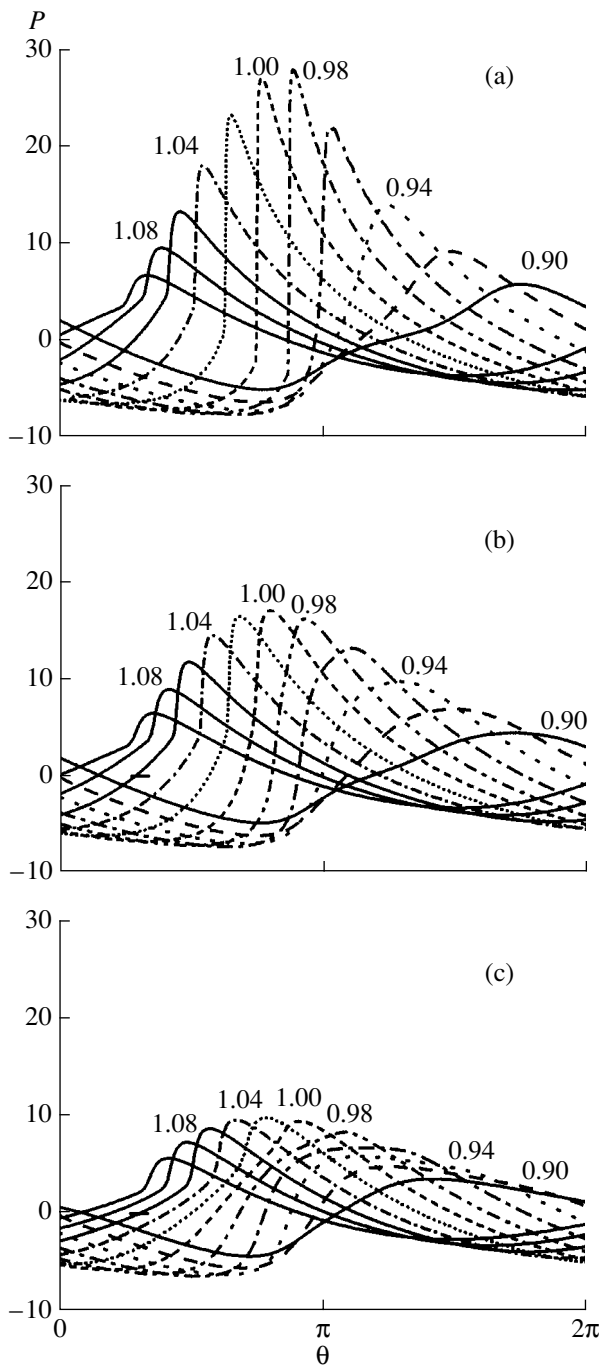


Fig. 2. Wave profiles in the focal region of the beam ($P = p/p_0$) in the case of a nonlinear mode of focusing at various distances from the radiator $Z = z/F$ (numbers at the curves) and from the beam axis: $R = r/r_0 =$ (a) 0, (b) 0.01, and (c) 0.02.

The following basic parameters of the scheme were used: the spatial window in the longitudinal coordinate $0.4 \leq Z \leq 1.6$, the spatial window in the transverse coordinate $0 \leq R \leq 0.2$, the grid step in the longitudinal coordinate $hZ = 2 \times 10^{-3}$, the grid step in the transverse coordinate $hR = 10^{-3}$, and the time step $ht = 1.5 \times 10^{-2}$.

INFLUENCE OF NONLINEAR EFFECTS ON ACOUSTIC FIELD CHARACTERISTICS AND ON TEMPERATURE DISTRIBUTION IN TISSUE

The results obtained from the simulation of Eqs. (1) and (15) provide an opportunity to investigate the influence of acoustic nonlinearity on the temporal and spatial characteristics of an ultrasonic beam, on the distribution of thermal sources, and on the evolution of the thermal field in the tissue. Figure 2 shows the profiles of an acoustic wave in the focal region at various distances along and across the beam axis, which are calculated with allowance for nonlinear effects. One can see that a shock front arises in the wave profile and the profile shape is characterized by a considerable asymmetry of the positive and negative phases. The positive peak value of the profile in the focus is almost three times as great as the peak value obtained under the approximation of linear wave propagation. The total pressure difference in the profile of a nonlinear wave is one and a half times greater than the corresponding value in the case of the linear wave propagation. One can also see that a considerable manifestation of nonlinear effects occurs only in a small spatial region near the focus: $r/r_0 = 0.02$, $0.95 < z/F < 1.05$, which corresponds to dimension scales of approximately 1.5 mm in the transverse direction and 1.5 cm in the longitudinal direction. One can expect a considerable increase in the efficiency of the tissue heating precisely in this region.

In the nonlinear mode of ultrasonic wave propagation in a tissue, the spectrum of the wave acquires new higher harmonics. Figure 3 presents the distributions of the amplitudes of the first three harmonics in a nonlinear beam (the solid curves 1, 2, and 3) and the distribution of the amplitude of the fundamental harmonic in the case of linear propagation (the dashed curve 1') in the focal plane and along the beam axis. One can see from these figures that the amplitudes of higher harmonics are sufficiently large and their spatial distributions in the focal region are narrower than the distributions for the fundamental frequency in both longitudinal and transverse directions.

As the frequency grows, the absorption increases. However, at the same time the diffraction effects become weaker and the beam focusing improves. Therefore, we can expect that near the focus, the total intensity of the wave calculated in the nonlinear case by the sum of the intensities of all harmonics differs from the intensity of the first harmonic obtained in the case of linear wave propagation. Figures 4 and 5 present the spatial distributions of the wave intensity and the power of thermal sources in the focal plane $z = F$ and along the beam axis for the linear (curves 1) and nonlinear (curves 2) modes of focusing. One can see that in the case of the nonlinear wave propagation, a small (about 15%) increase in the amplification factor in the focus is observed along with an improvement of the spatial localization of the beam in comparison to the linear

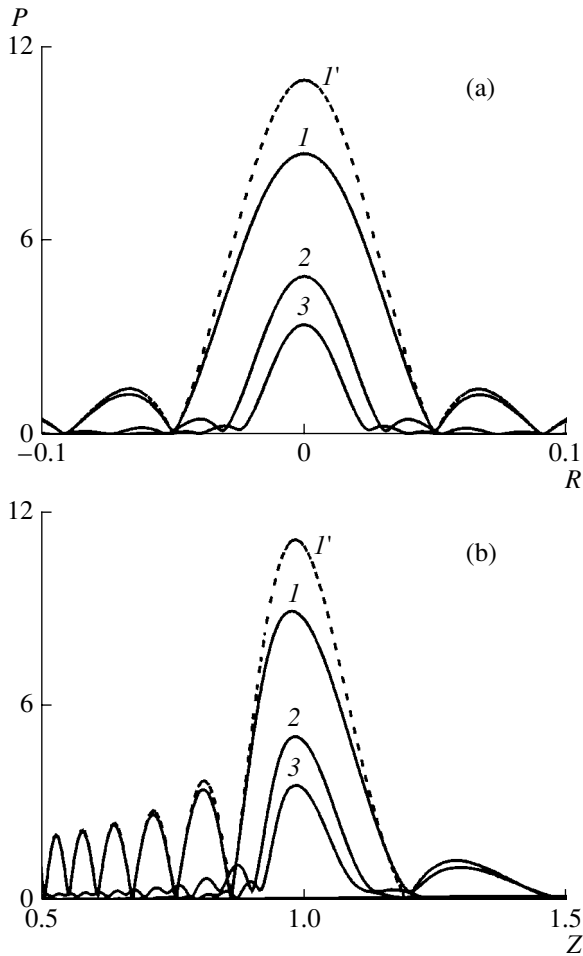


Fig. 3. Spatial distributions of the pressure amplitudes of the first three harmonics $P = 2|C_n|$, $n = (1)$ 1, (2) 2, and (3) 3 in a nonlinear beam and (I') the amplitudes of the fundamental harmonic in the case of linear propagation: (a) in the focal plane $z|F| = 1$ and (b) along the beam axis.

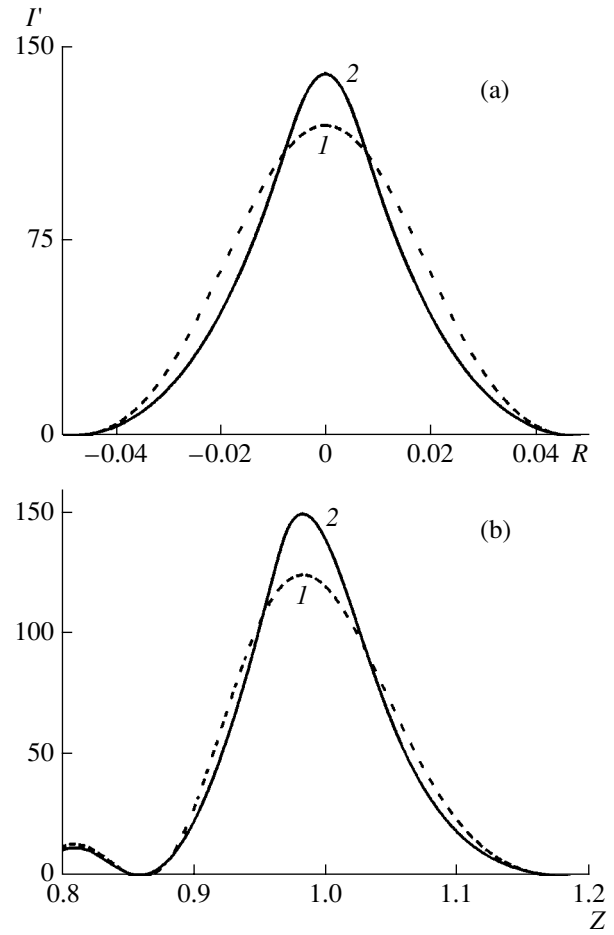


Fig. 4. Spatial distributions of the total intensity $I' = I/I_0$ (a) in the focal plane and (b) along the beam axis for the (1) linear and (2) nonlinear modes of focusing.

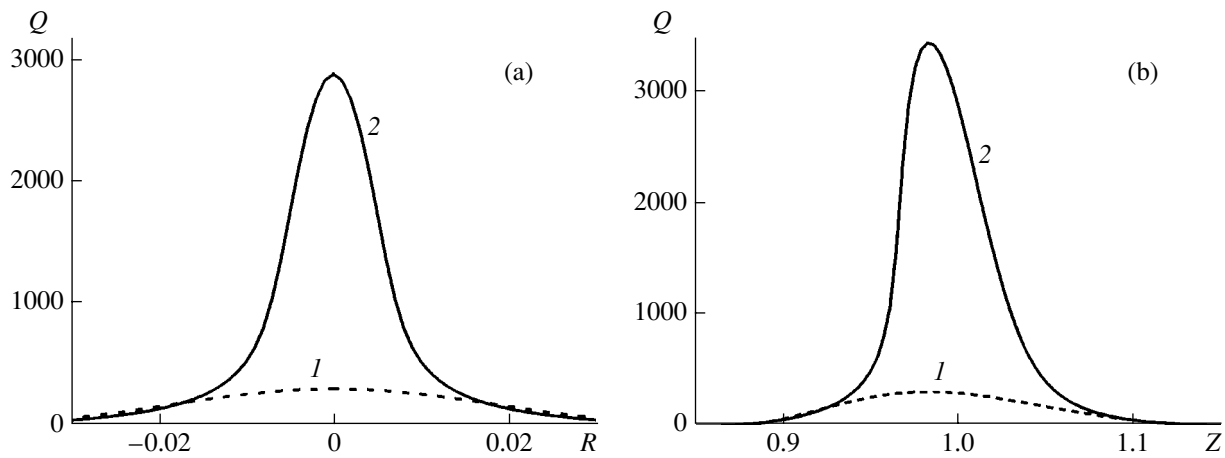


Fig. 5. Distributions of thermal sources $Q = q/q_0$ (a) in the focal plane and (b) along the beam axis for the (1) linear and (2) nonlinear modes of focusing.

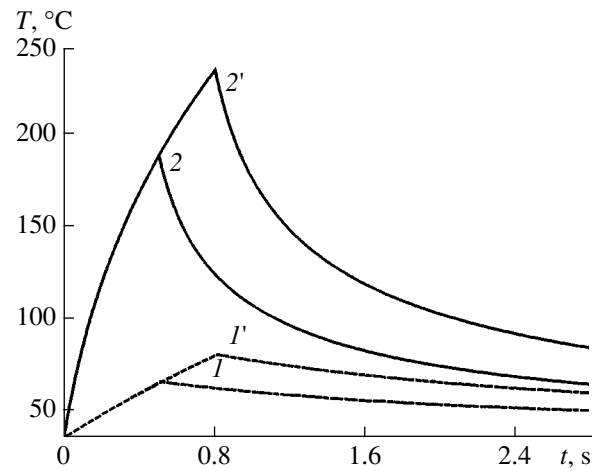


Fig. 6. Dependences of temperature on time in the focus for the (1) linear and (2) nonlinear modes of focusing and for different times of irradiation: (1, 2) 0.5 and (1', 2') 0.8 s.

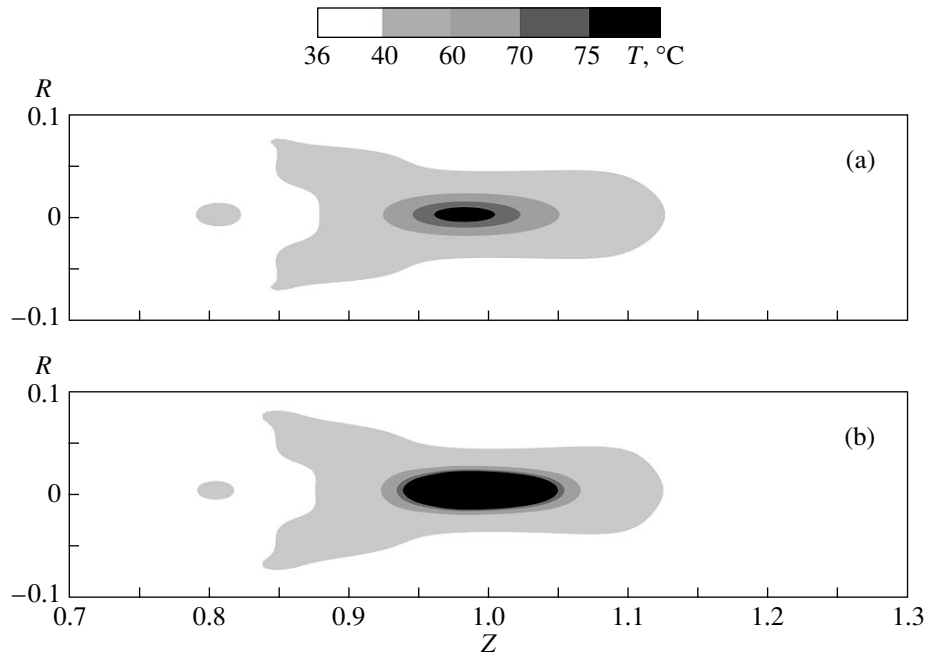


Fig. 7. Spatial temperature distributions in the focal region for the (a) linear and (b) nonlinear modes of focusing in the case of the irradiation time 0.8 s.

case. At the same time, the nonlinear effects lead to a considerable increase in the power of thermal sources in the focal region of the beam. The efficiency of heating increases by almost an order of magnitude, which agrees with the theoretical estimates given above. Thus, the intensity used is close to optimal in terms of the realization of the mode of local tissue heating in the focus due to the absorption at shock fronts. A shock arises close to the focus, and, therefore, one obtains no additional losses of wave energy and no increase in heating in the prefocal region.

Figure 6 shows the dependences of temperature on time in the focus for the linear (curves 1) and nonlinear

(curves 2) modes of focusing with the exposures 0.5 and 0.8 s. As one can see, even with that short irradiation times, the diffusion of heat manifests itself quite strongly and the dependence $T(t)$ differs from the linear one. The high spatial gradient in the distribution of thermal sources in the nonlinear mode (Fig. 5) amplifies the diffusion process. Therefore, despite the fact that the power of thermal sources in the focus for the linear and nonlinear modes of heating differs by an order of magnitude, the increase in temperature differs by only a factor of three.

Figure 7 illustrates the two-dimensional spatial distributions of temperature calculated for the irradiation

time 0.8 s in the linear and nonlinear modes of wave propagation. One can see that in the case of the nonlinear mode, the region of strong heating (over 75°C) is considerably wider in both longitudinal and transverse directions and shifted slightly towards the radiator. In contrast, the region with moderate temperature in the case of the nonlinear propagation is narrower than in the linear mode, which is caused by a better localization of heating.

CONCLUSIONS

The theoretical approach, the numerical algorithm, and the computer codes developed in this study provide an opportunity to effectively investigate the problems of focusing of a high-intensity acoustic beam in a biological tissue and the corresponding tissue heating in the conditions of strong manifestation of the effects of acoustic nonlinearity. A numerical simulation of the acoustic and temperature fields in a biological tissue is conducted for the conditions characteristic of real clinical setups used in ultrasonic surgery. The predictions made with the use of two models, which do and do not take into account the acoustic nonlinearity of the tissue, are compared. It is demonstrated that nonlinear effects lead to an increase in the power of thermal sources in the focus by approximately an order of magnitude and to a certain improvement of the locality of heating. The heat diffusion in the tissue leads to smoothing of the spatial distribution of temperature compared to the distribution of thermal sources, the diffusion processes being more pronounced in the nonlinear mode of focusing. With the acoustic nonlinearity taken into account, the maximal temperature increment in the focus several times exceeds the value obtained in the approximation of linear wave propagation; i.e., the role of nonlinear processes is of fundamental significance.

ACKNOWLEDGMENTS

We are grateful to Dr. G.R. Ter Haar for supporting the idea to conduct this study and to Dr. O.A. Sapozhnikov for useful discussions. The work was supported in part by the Russian Foundation for Basic Research (project no. 98-02-17318) and the Civilian Research and Development Foundation for the independent states of the former Soviet Union (project no. RP2-2099).

REFERENCES

1. J. G. Webster, *Wiley Encyclopedia of Electrical and Electronics Engineering* (Wiley, 1999), pp. 368–386.
2. *Physical Principles of Medical Ultrasonics*, Ed. by C. R. Hill (Ellis Horwood, Chichester, 1986; Mir, Moscow, 1989).
3. G. R. Ter Haar, I. H. Rivens, E. Moskvic, *et al.*, Proc. SPIE **3249**, 270 (1998).
4. J. Y. Chapelon and D. Cathignol, in *Advances in Nonlinear Acoustics: Proceedings of the 13th International Symposium on Nonlinear Acoustics* (Bergen, Norway, 1993), pp. 21–29.
5. M. F. Hamilton and D. T. Blackstock, *Nonlinear Acoustics* (Academic, Boston, 1998), p. 139.
6. V. A. Khokhlova, O. A. Sapozhnikov, and L. A. Crum, J. Acoust. Soc. Am. **102**, 3155 (1997).
7. P. Meaney, M. D. Cahill, and Gail ter Haar, Proc. SPIE **3249**, 246 (1998).
8. F. P. Curra, P. D. Mourad, V. A. Khokhlova, and L. A. Crum, in *Proceedings of the IEEE International Ultrasonics Symposium* (Sendai, Japan, 1998), pp. 1419–1422.
9. N. S. Bakhvalov, Ya. M. Zhileikin, and E. A. Zabolotskaya, *Nonlinear Theory of Sound Beams* (Nauka, Moscow, 1982; AIP, New York, 1987).
10. Y. S. Lee and M. F. Hamilton, J. Acoust. Soc. Am. **97**, 906 (1995).
11. J. Tavakkoli, D. Cathignol, R. Souchon, and O. A. Sapozhnikov, J. Acoust. Soc. Am. **104**, 2061 (1998).
12. Tjotta Naze, S. Tjotta, and E. H. Vefring, J. Acoust. Soc. Am. **88**, 2859 (1990).
13. T. S. Hart and M. F. Hamilton, J. Acoust. Soc. Am. **84**, 1488 (1988).
14. P. T. Christopher and K. J. Parker, J. Acoust. Soc. Am. **90**, 488 (1991).
15. Yu. A. Pishchal'nikov, O. A. Sapozhnikov, and V. A. Khokhlova, Akust. Zh. **42**, 412 (1996) [Acoust. Phys. **42**, 362 (1996)].
16. V. A. Khokhlova, M. A. Averkiou, S. J. Younghouse, M. F. Hamilton, and L. A. Crum, in *Proceedings of 16th ICA/135th ASA Meeting* (Seattle, USA, 1998), Vol. 4, p. 2875.
17. S. S. Kashcheeva, V. A. Khokhlova, O. A. Sapozhnikov, *et al.*, Akust. Zh. **46**, 211 (2000) [Acoust. Phys. **46**, 170 (2000)].
18. V. M. Paskonov, V. I. Polezhaev, and L. A. Chudov, *Numerical Simulation of the Processes of Heat and Mass Transfer* (Nauka, Moscow, 1984).
19. W. L. Nyborg, Phys. Med. Biol. **33**, 785 (1988).

Translated by M. Lyamshev

